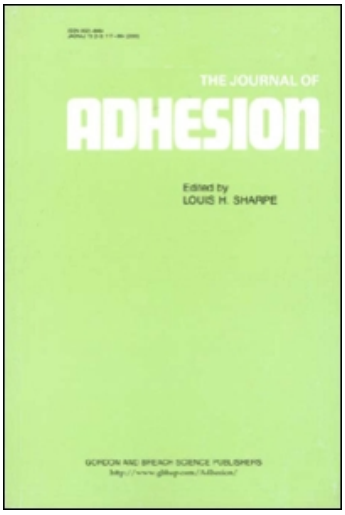

The Journal of Adhesion
Publication details, including instructions for authors and subscription information:
http://www.informaworld.com/smpp/title~content=t713453635

Hydrothermal Aging of Composite Materials Part 2: Matrix Aspects

D. H. Kaelble[a]; P. J. Dynes[a]
[a] Science Center. Rockwell International, Thousand Oaks, California, U.S.A.

To cite this Article Kaelble, D. H. and Dynes, P. J.(1976) 'Hydrothermal Aging of Composite Materials Part 2: Matrix Aspects', The Journal of Adhesion, 8: 3, 195 — 212
To link to this Article: DOI: 10.1080/00218467608075083
URL: http://dx.doi.org/10.1080/00218467608075083

J. Adhesion, 1977, Vol. 8, pp. 195–212

Printed in Scotland

Hydrothermal Aging of Composite Materials

Part 2: Matrix Aspects

D. H. KAELBLE and P. J. DYNES

Science Center, Rockwell International, Thousand Oaks, California 91360, U.S.A.

(*Received December 22, 1975*)

The effects of hydrothermal (100°C in H_2O) aging on the epoxy matrix phase of a graphite–epoxy composite is examined in terms of chemical structure and rheological response. Infrared spectra indicate the resin system is a dicyandiamide (DICY) cured diglycyl ether of Bisphenol-A (DGEBA). Hydrothermal aging is shown to modify the resin network structure and increase the magnitude of the low-temperature β transition in short range molecular motion where $T_\beta \simeq -45 \pm 15$°C at frequencies of 3.5 to 110 Hz. In addition to network structure changes the absorbed moisture temporarily lowers the resin glass temperature so that at 100°C in water the resin exhibits a rubbery response state. Evaluation of fracture properties of aged resin shows a loss in fracture toughness and development of internal microcracks in the bulk resin during hydrothermal aging.

INTRODUCTION

A number of studies of hydrothermal aging of graphite fiber reinforced composites show that moisture degradation can substantially diminish interlaminar shear strength and modify fracture toughness.[1-5] Earlier studies apparently have not been concerned with the consequences of hydrothermal aging upon the chemical structure and physical properties of the polymeric matrix component of the reinforced composite material.

This discussion forms a second part of a detailed study of hydrothermal (100°C in H_2O) aging in composite materials.[5] The effect of the fiber-matrix interfacial bond was emphasized in Part I and here the chemistry and physics contributions of the matrix phase on hydrothermal aging processes is emphasized. In this phase of the investigation hydrothermal aging cycles were

applied to the pure epoxy matrix without fiber reinforcement in an effort to isolate the matrix aspect of composite degradation.

MATERIALS AND METHODS

The epoxy resin system BP907 (Bloomingdale Division of American Cyanamid) was obtained as a one-part system with epoxy and curative components premixed and dispersed in methylene chloride. One of the primary advantages of BP907 is the long term storage stability of the uncured material (up to 6 months at 23°C). This resin system requires a high temperature for cure (1 hour at 170°C to 177°C) as described by manufacturer's recommendations. In all studies with this system the methylene chloride component of BP907 was removed prior to curing by vacuum drying of cast films at mild heat, $T \leqslant 60$°C. In general, curing was accomplished by providing a final curing condition of 2 hours at 170°C unless otherwise specified.

The chemical aspects of curing and hydrothermal aging of BP907 cast films were evaluated by differential scanning calorimetry (Perkin–Elmer DSC–1B®) and infrared spectroscopy (Beckman Spectrophotometer IR4250®). Differential scanning calorimetry (DSC) provides a nearly ideal tool for quantitative assessment of the kinetics of curing by direct measurement of the heat of polymerization ΔH_p and the rate of curing in terms of dH_p/dT at constant thermal scan rate $\phi = dT/dt$. DSC measurements for heat capacity change in the cured BP907 is also applied to determine the glass (glass to rubber) transition temperature T_g.

The rheological effects of hydrothermal aging of BP907 films were measured through the tensional dynamic modulii:

$$E^* = E' + iE'' \tag{1}$$

and loss tangent:

$$\tan \delta = E''/E' \tag{2}$$

where E^* is the complex dynamic Young's modulus E' the storage (in-phase) component, and E'' is the loss (out-of-phase) component. These properties were measured at constant frequency $f = 3.5$, 11, 35 and 110 Hz under varying temperature using the Rheovibron DDV–II–C (Toyo Baldwin Co. Ltd.).

Thermomechanical analysis (TMA) measurements are also applied to characterize the extension-recovery response of hydrothermally aged BP907. TMA measurements apply a repetitive cycle of extension-recovery to a microtensile specimen (ASTM Method D1708–66) while temperature varies at a uniform rate $\phi = 1.0$°C/min. The maximum strain amplitude $\varepsilon = \Delta L/L_0 \leqslant 0.01$ at constant strain rate $\dot{\varepsilon} = \pm 0.022\ \text{min}^{-1}$ is automatically imposed by an Instron TM–M–L machine. Between extension-recovery cycles the Instron

is programmed to maintain the net force on the sample at $F = 0$. The mechanical response properties measured by TMA include the tensile relaxation modulus $E(t)$ at constant strain rate $\dot{\varepsilon}$ as follows:

$$E(t) = \frac{d\sigma(t)}{d\varepsilon} = \frac{d\sigma(t)}{\dot{\varepsilon}\, dt} \tag{3}$$

where $\sigma(t)$ is time dependent stress at time t where $t = 0$ when $\varepsilon = 0$.

MECHANISMS OF CURING

A significant portion of the total hydrothermal aging history of an epoxy–graphite composite is, of course, the curing cycle and the chemical reactions which convert the matrix from the initial compliant bonding state to the final solid holding state. The solidification of the resin matrix during cure is produced by the increase in the glass transition temperature T_g which accompanies the chemical reactions that crosslink and polymerize the resin

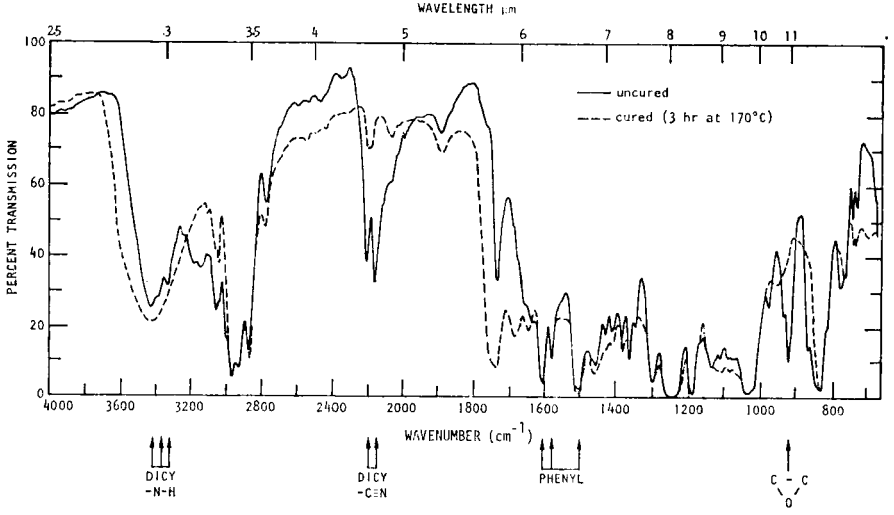

FIGURE 1 Infrared spectra for uncured and cured films of BP907 epoxy matrix on NaCl crystal.

phase. The IR adsorption spectrum for uncured and cured (3 hours at 170°C) films of BP907 epoxy are shown in Figure 1. The IR spectrum of the uncured BP907 indicates this matrix system contains the epoxy and curative structures shown in Table I. Reference IR spectrum for the uncured DGEBA epoxy of Table I is given by Lee and Neville[6] and for the DICY curative by Wagner.[7] Inspection of Figure 1 shows that the IR adsorption at 920 cm^{-1} for the

epoxy group of DGEBA and the nitrile adsorption at $\simeq 2200\,cm^{-1}$ and amine adsorption at $\simeq 3400\,cm^{-1}$ wave number for DICY are not present in the IR spectrum of the cured BP907. This result coincides with the mechanism for DICY curing of epoxy resins proposed by Saunders, Levy and Serino[8] and outlined in Table II. The reaction mechanism of Table II proposes that the first crosslinking reaction involves the epoxy ring opening

TABLE I

Suggested coreactants in Epoxy BP907 resin

Epoxy: diglycidyl ether of bisphenol-A (DGEBA); M.W. $\simeq$ 370–400 gm/mole

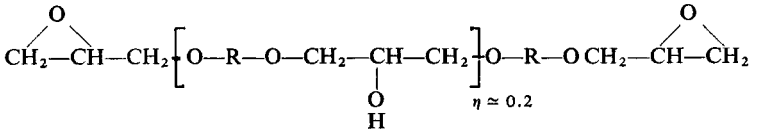

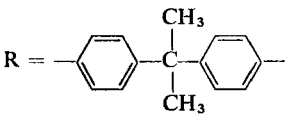

Curative: dicyandiamide (DICY); M.W. $\simeq$ 84 gm/mole

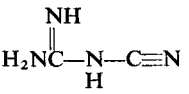

and crosslinking through the active hydrogen of the amino ($—NH_2$) and imino ($=NH$) groups in the DICY curative. A second reaction is postulated in Table II to involve the addition of hydroxyl hydrogen across the nitrile triple bond to produce the guanyl urea. This second reaction modifies the structure of the crosslinked unit formed between DGEBA epoxy and DICY.

Lewis and Saxon[9] point out that DICY, with a crystalline melting point $T_m = 211°C$, is insoluble in the DGEBA epoxy at room temperature. The finely ground DICY is suspended in the epoxy. This solid DICY suspension goes into solution in the epoxy and reacts at temperatures of 100°C or higher to crosslink the epoxy phase. It might be expected that the combined process of physical solution and chemical reaction of DICY in epoxy resin would lead to complicated reaction kinetics. The DSC thermogram for the curing of BP907 at scan rate $\phi = 10°C/min$ given in the upper solid curve of Figure 2 shows that curing initiates at $T_I = 157°C$ achieves a maximum rate at $T^* = 192°C$ and is completed at $T_c = 237°C$. Integration under the dH_p/dT versus

TABLE II

Suggested curing mechanism for epoxy BP907 resin

Epoxy+Dicyandiamide (DICY)

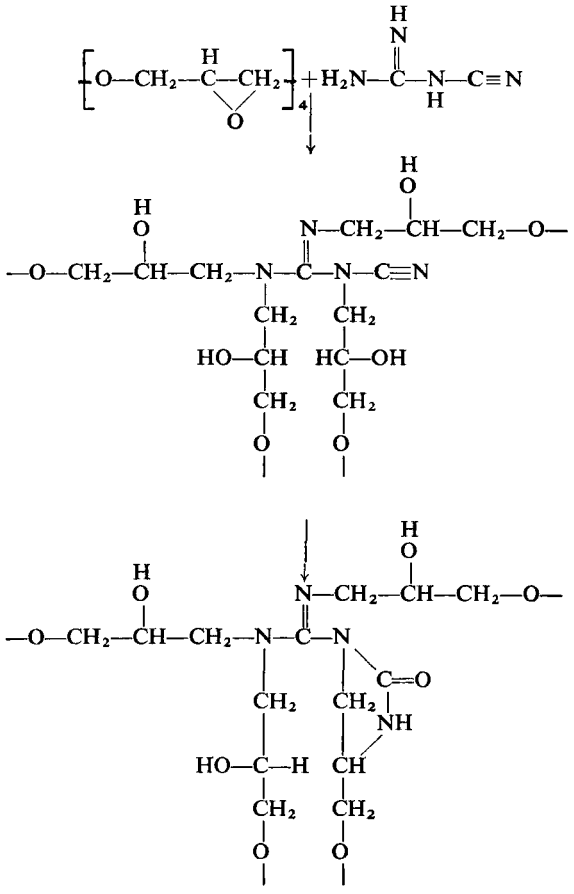

T curve identifies a total heat of polymerization of $\Delta H_p = 73.1$ cal/gm for BP907. The dashed curve of upper Figure 2 identifies the unreacted fraction $(1-x)$ of crosslinking units as a function of temperature as defined by partial integration of the DSC thermogram. The lower curve of Figure 2 shows a characteristic DSC scan of the cured BP907 where the change in heat absorption rate dH/dt versus T describes a specific heat change characteristic of a glass transition range $T_g \simeq 122 \pm 15°C$ where T_g is the inflection point in the DSC curve. It is evident from the curves of Figure 2 that BP907 is always in

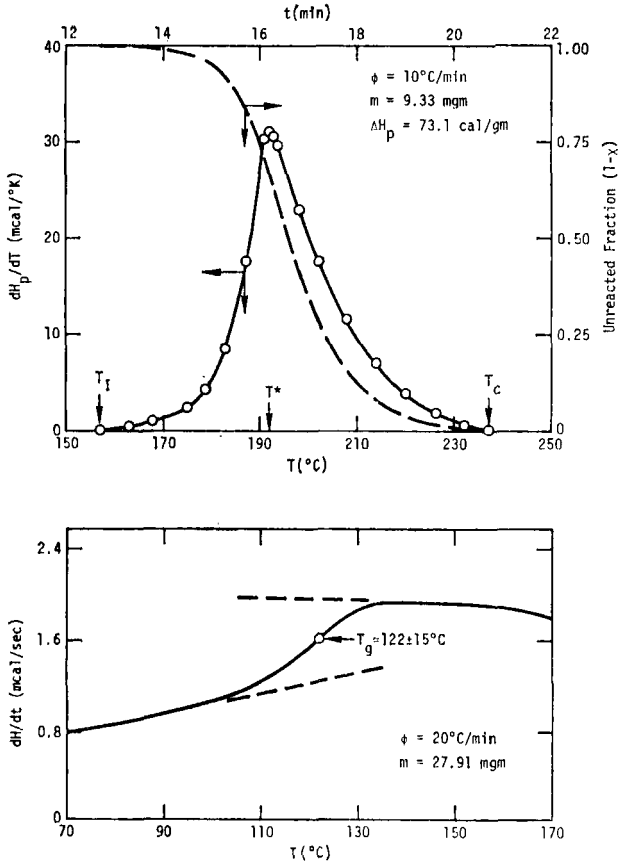

FIGURE 2 Kinetics of curing (upper view) and glass transition of cured BP907 (lower view) as measured by DSC.

a liquid or rubbery state while curing since $T_g \simeq 122°C$ for the fully cured resin is below $T_I = 157°C$ where the cure reaction initiates.

Attempts to analyze the kinetics of curing of BP907 by analysis of DSC curves as shown in upper Figure 1 by standard methods[10-12] designed to isolate parameters such as kinetic order of reaction n and apparent activation energy of curing E were unsuccessful. The DSC kinetics analysis assumes constant initial concentration of reactants. Evidently this assumption does not correlate with the variable reactant concentration introduced by the gradual melting and co-solution of DICY in the epoxy phase with increased temperature. The other major complication to chemical kinetics analysis produced by change from liquid to glass state during cure is not present with BP907 since $T_I < T_g$ as mentioned above.

As pointed out by Kenyon and Neilsen[13] the properties of epoxy resins depend upon the uniformity of the network structure which can vary with curing conditions and chemical constitution. Recent gel permeation chromatography (GPC) studies by Screaton and coworkers[14] show that commercial DGEBA epoxy monomers are complex mixtures of reactive monomers. Cured samples of BP907 resin showed equilibrium weight gain of 11.2 ± 0.9 pbw (part by weight) of H_2O after long term (50 to 150 hours) hydrothermal aging (H_2O at 100°C). Subsequent desiccation of these samples showed a total weight loss of extractible BP907 of less than 2%. The number average molecular weight M_x between effective crosslinks is defined from the kinetic theory of rubber elasticity by the following relation[15]:

$$M_x = 3\rho RT/E_i(t) \tag{4}$$

where ρ is polymer density $R = 84.8$ kg cm/mole deg. is the gas constant and T is the absolute temperature. From TMA measurements of cured BP907 in the equilibrium rubbery state of response a value for the tensile relaxation modulus $E_i(t) = 126$ kg/cm^2 at $T = 150$°C $= 423$°K where $\rho \simeq 1.21$ gm/cc we calculate a value of $M_x = 1033$ gm/mole. The epoxy and curative structures and reaction chemistry described in Table I and Table II provides a theoretical $M_x = 407 \pm 15$ gm/mole for an ideal BP907 crosslinked network. A similar ratio of $M_x(\text{exp})/M_x(\text{theor.}) \simeq 2.0$ to 2.5 has been shown in other studies[13, 15] and appears to indicate the possibility of a heterogeneous network with regions of higher and lower crosslinking in cured BP907 resin.

CHEMISTRY OF HYDROTHERMAL AGING

Additional long term studies of heat aging effects on BP907 reveal that subtle but important changes in chemical structure and properties continue after cure. Films of BP907 were cured for 2 hours at 170°C according to the manufacturer's recommended cycle. The effects of subsequent aging are shown in Figure 3 by the IR spectrum for aging in H_2O (left view) and dry N_2 (right view) which shows the further slow disappearance of the cyano adsorbance at wavenumber $\simeq 2190$ cm^{-1}. The structure changes for both wet and dry aging of cured BP907 at 100°C indicated by Figure 3, appear to coincide with the lower reaction of Table II wherein the nitrile (—C≡N) disappears through formation of a guanyl urea ring structure.

The conversion of the crosslink structure indicated by the data of Figure 3 and the lower reaction of Table II might be expected to modify the thermally activated local motion in the solid state of the BP907 resin. There now exists a general proposition that polymers display a number of significant thermal transitions of motion in the amorphous solid state.[16] These multiple transitions are now denoted α, β, γ, δ, etc. in their appearance on a descending

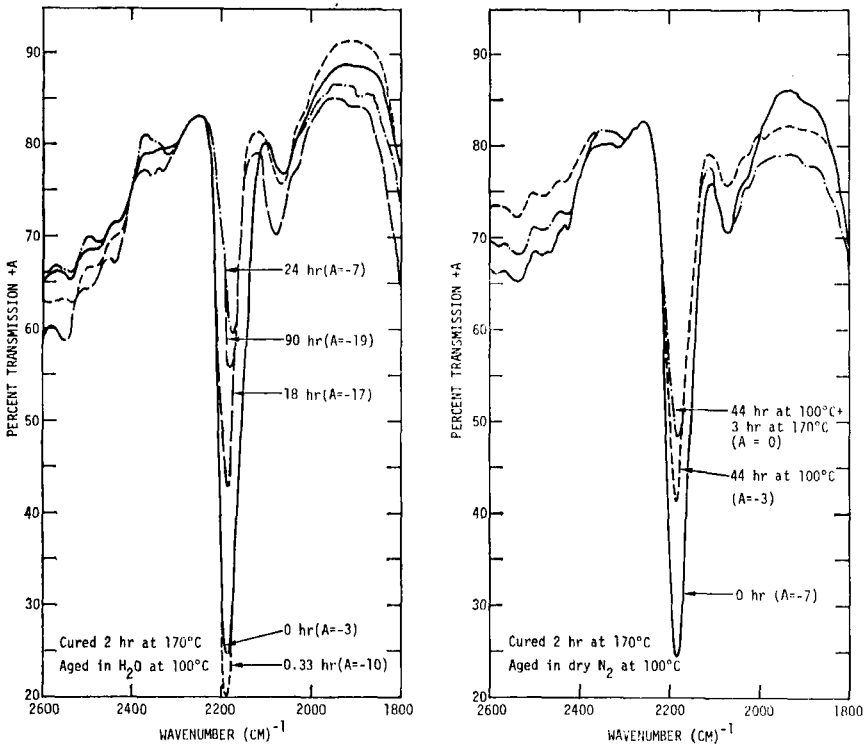

FIGURE 3 Infrared spectra of cured BP907 epoxy at varied exposures to hydrothermal (left view) and dry thermal aging (right view).

temperature scale. The α transition is associated with T_g and the major glass-to-rubber transition in high polymers. In amine cured epoxy resins based upon DGEBA such as BP907 a prominent β transition is recognized to involve the glycidyl ether portion of the molecule as follows[15]:

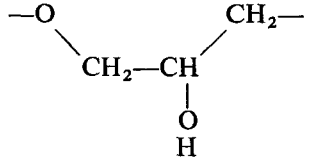

which forms a crankshaft rotor. Kline[17] recognized this β transition in cured epoxies at $-33°C$ at frequencies of 300 to 1300 Hz, whereas May and Weir[18] observed equivalent transitions at $-60°C$ using a frequency of 1.0 Hz in dynamic mechanical measurements. As shown in Table II, four of the above segments are produced by DICY curing and one of these glycidyl ether segments is modified to a ring structure in the second reaction. Thermal scans

of cured and unaged (virgin) BP907 resin at temperatures from −150°C to 50°C were run at frequencies of $f = 3.5$, 11, 35 and 110 Hz on the Rheovibron so to characterize dynamic mechanical loss tan δ through the β transition. The BP907 sample was then hydrothermally aged (100°C in H_2O) for 60 hours to achieve 8.1 pbw H_2O and subsequently desiccated. The Rheovibron scan was then repeated on the aged and dried specimen. The effects of hydrothermal aging on the β transition of BP907 is shown by the tan δ versus T functions shown in Figure 4 through Figure 7 for respective scan frequencies $f = 3.5$, 11, 35 and 110 Hz. The immediately apparent effect of hydrothermal aging as shown in the curves of Figure 4 through Figure 7 is a generalized increase in the maximum tan δ value for the β transition and a broadening shift of tan δ values to higher temperature at $T > T_\beta$ where T_β denotes the temperature where tan δ maximizes. Inspection of Figure 4 through Figure 7 also shows that T_β is systematically shifted to higher temperature with increased test frequency f in both virgin and aged BP907 epoxy.

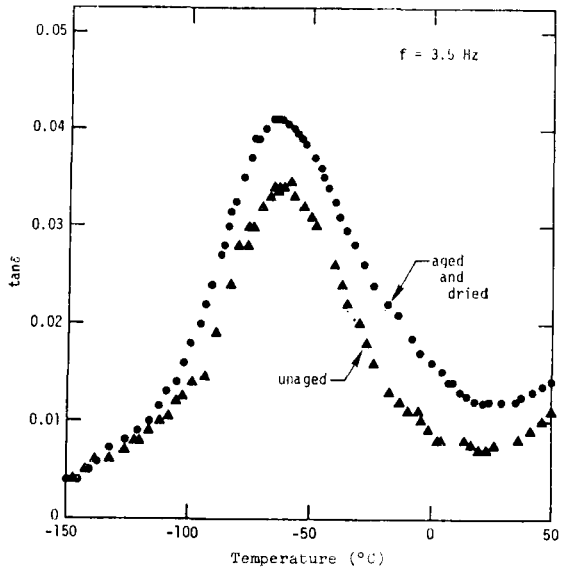

FIGURE 4 Temperature dependence of loss tangent for BP907 at 3.5 Hz.

It is found in polymeric systems that the frequency-temperature shift of β, γ, δ transitions of the amorphous solid state often conform to a standard Arrhenius relation[16]

$$\ln a_T = \ln \frac{f_0}{f_T} = \frac{H}{R}\left(\frac{1}{T} - \frac{1}{T_0}\right) \tag{5}$$

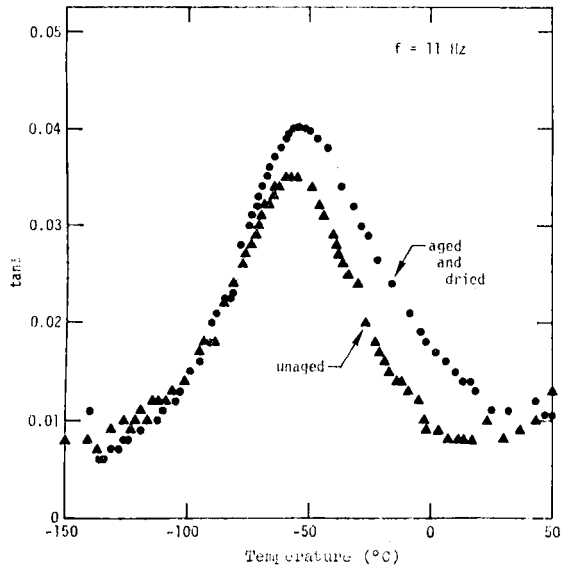

FIGURE 5 Temperature dependence of tan δ for BP907 at 11 Hz.

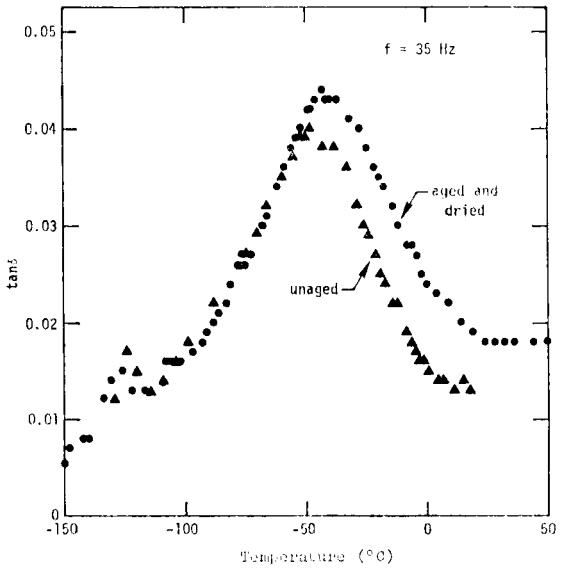

FIGURE 6 Temperature dependence of tan δ for BP907 at 35 Hz.

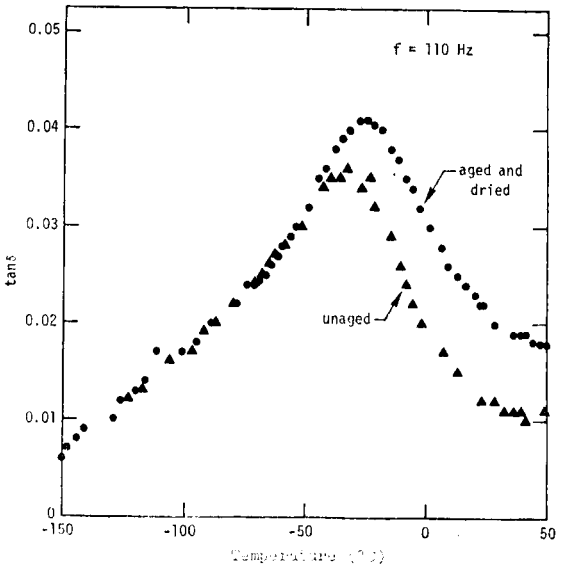

FIGURE 7 Temperature dependence of tan δ for BP907 at 110 Hz.

Alternatively, the α transition characterizing glass-to-rubber transformation at T_g is characterized by an equation of William, Landel and Ferry (WLF)[16]:

$$\ln a_T = \frac{-C_1(T-T_0)}{C_2+(T-T_0)} \tag{6}$$

where H in Eq. (5) is the apparent activation energy of viscous flow and C_1 and C_2 are empirically determined constants which relate to free volume changes, f_T and f_0 are the respective frequencies at test temperature T and

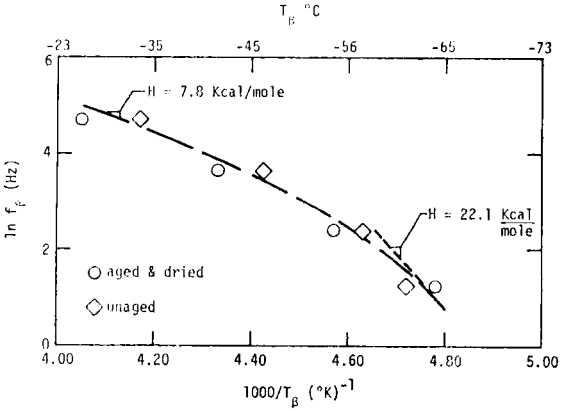

FIGURE 8 Frequency f_β versus temperature T_β dependence for BP907 damping maximum in the β (beta) transition region.

reference temperature T_0 in Kelvin units. Plots of $\ln f$ versus T_β^{-1}, as shown in Figure 8, indicate that the activation energy of Eq. (5) is probably a variable which ranges from $H \simeq 22.1$ at $T_\beta \simeq -65°C$ to $H \simeq 7.8$ kcal/mole at $T_\beta \simeq -30°C$ for the β relaxation of both unaged and hydrothermally aged BP907 epoxy.

A larger β transition is displayed by the hydrothermally aged BP907 epoxy as indicated by the larger areas beneath the tan δ versus T curves of Figure 5 through Figure 8. The increase in tan δ_β for aged BP907 is readily associated with increased molecular motion. The information conveyed by the IR spectra of Figure 3 would suggest that the glycidyl ether segments:

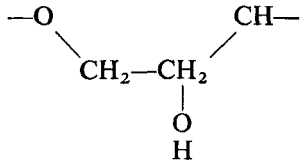

are partially replaced by the following segment:

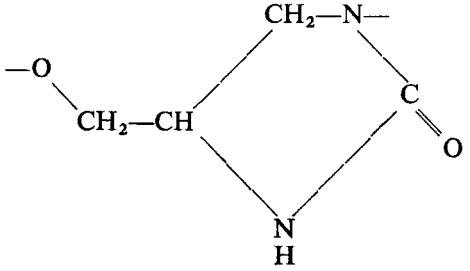

which being bulkier will enhance the β transition and probably display onset of rotational motion at higher temperature than the glycidyl ether segment it replaces.

The IR data of Figure 3 appear to couple well with the Rheovibron data of Figures 4–8 to show that specific structure rearrangements in the crosslink network modify and enhance the β transition of the crosslinked epoxy. The predicted result is that hydrothermal aging should lower the Young's modulus of cured BP907 at all temperatures above T_β since high tan δ is associated with a complementary modulus decrease with increased temperature or decreased frequency.

THERMOCHEMICAL RESPONSE

The mechanisms of matrix curing and hydrothermal aging influence composite response mostly through the changes they produce in resin modulus and strength. The three curves of Figure 9 graph the values of the tensile relaxation

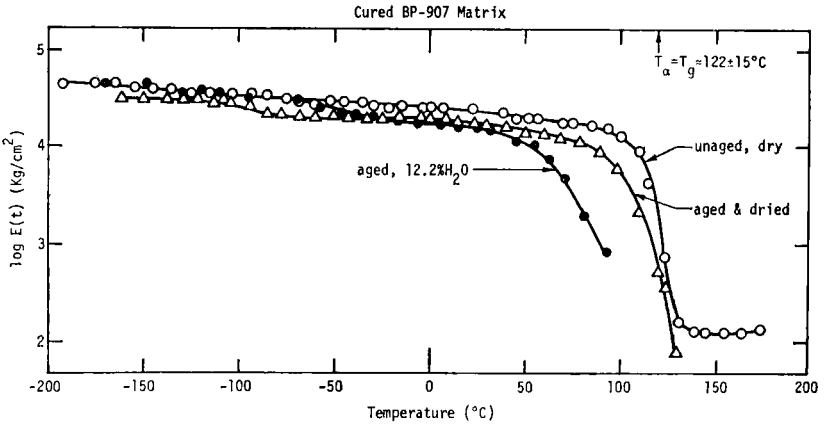

FIGURE 9 Tensile relaxation modulus $E(t)$ versus temperature T for BP907 at $t = 15$ sec.

modulus $E(t)$ determined for cured BP907 under the hydrothermal (100°C in H_2O) aging conditions detailed in Table III. The curves of Figure 9 illustrate that hydrothermal aging does enhance a change in $E(t)$ in the region of the β transition at temperatures $T = -100$ to -50°C. As shown by Table III, this aging effect tends to reduce the value of $E(t)$ at 25°C for both hydrated and desiccated BP907 epoxy. The curves of Figure 9 and data of Table III thus show that room temperature tensile modulus is irreversibly reduced by hydrothermal aging. This result is, of course, consistent with the IR and Rheovibron data discussed in relation to the chemistry of aging.

TABLE III

Effects of hydrothermal aging (100°C in H_2O) on the tensile relaxation modulus $E(t)$ of cured BP907 epoxy

Aging condition Test temperature (°C)	Virgin, dry	Aged 60 hr, 12.2% H_2O $E(t)$ (kg/cm^2)	Aged 60 hr, then dried
−150	$3.89 \cdot 10^4$	$4.46 \cdot 10^4$	$3.09 \cdot 10^4$
25	$2.29 \cdot 10^4$	$1.66 \cdot 10^4$	$1.66 \cdot 10^4$
150	$1.26 \cdot 10^2$	—	—
remarks	no failure	sample broke at $\epsilon \leqslant 0.01$ and $T = 92$°C	sample broke at $\epsilon \leqslant 0.01$ and $T = 130$°C

The curves of Figure 9 also show that in the glass-to-rubber transition region the presence of 12.2 pbw water of solution in hydrothermally aged BP907 appear to reduce T_g by about 50°C. In other words water is an effective

temporary plasticizer of the molecular motions which dominate T_g response. Subsequent drying, as Figure 9 shows, shifts the $E(t)$ versus T curve nearly back to the temperature shown by the alpha transition for unaged specimen. Thus, the effects of moisture exposure on the alpha transition response of BP907 appear to be much more reversible than shown for beta transition response.

As noted in the remarks column of Table III the TMA study for both the aged-wet and aged-dried samples of BP907 terminated in tensile failure at low strain $\varepsilon \leqslant 0.01$ in the alpha transition region where rubbery response dominates. To investigate this phenomenon further a series of TMA test specimens were prepared, hydrothermally aged and then tested in both wet and dried states. A summary description of aging conditions and room temperature tensile fracture properties are presented in Table IV. Sample

TABLE IV

Effects of hydrothermal aging (100°C in H_2O) on the tensile strength σ_b, extensibility ϵ_b, and specific fracture energy W_b/V of cured BP907

Aging condition	Virgin, Dry	Aged 132 hr, 12.1% H_2O	Aged 132 hr, then dried
Test temperature	23	23	23
Number of tests	7	7	6
σ_b (kg/cm^2)	772±26	322±18	472±20
$100\epsilon_b = 100(\Delta L/L_0)$	6.15±0.70	2.64±0.27	3.48±0.22
W_b/V (kg cm/cm^3)	31.2±5.5	4.58±0.76	7.96±0.86

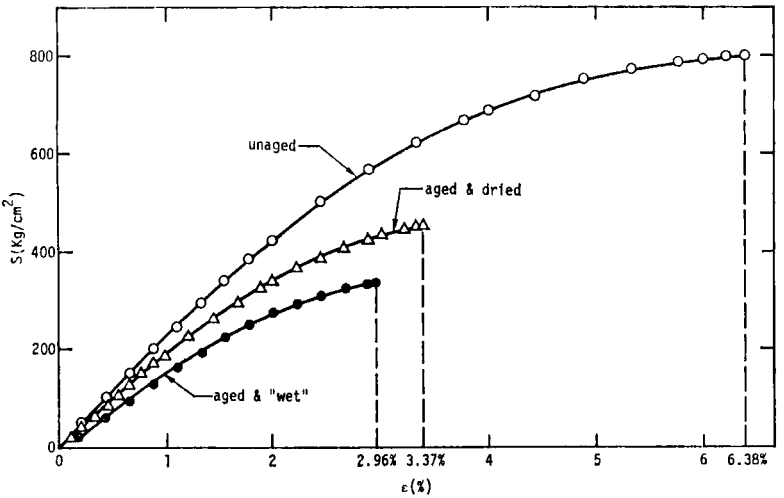

FIGURE 10 Tensile deformation and fracture response of BP907 epoxy.

geometries and strain rate described for TMA were applied in these tests and typical stress-strain curves for the unaged and two aged materials are graphed in Figure 10. One notes in Figure 10 that room temperature testing of cured BP907 epoxy immediately upon removal from 132 hours of hydrothermal aging shows equal reductions in both tensile strength and extensibility by 58%. Subsequent desiccation of the aged samples shows only a fractional recovery of 18% in strength and 15% in extensibility toward original averaged values of $\sigma_b = 772\ \text{kg/cm}^2$ and $\varepsilon_b = 6.15 \cdot 10^{-2}$. The greatest fractional loss

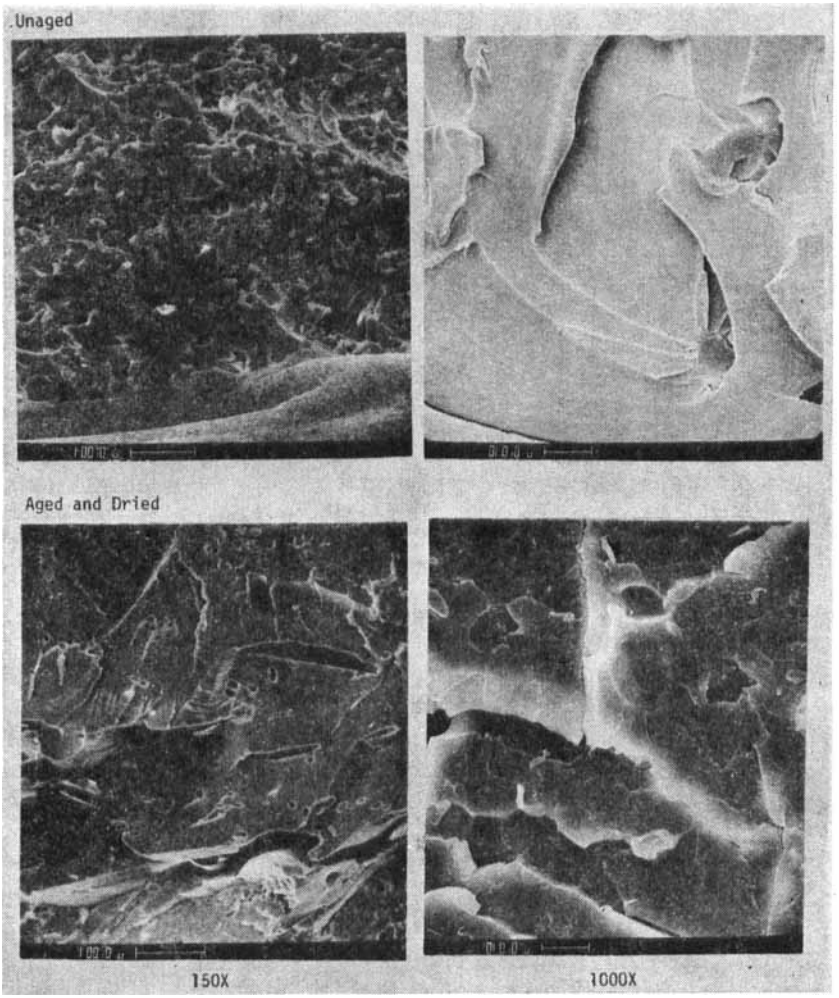

FIGURE 11 Tensile fracture surfaces for unaged (upper views) and aged and dried BP907 (lower view).

of mechanical response is shown in Table IV to appear in the specific fracture work (W_b/V) where W_b is defined as a maximum value of tensile work at fracture and $V = A_0 \cdot L_0$ = sample volume in the strained gage length L_0. The magnitude of W_b/V relates to the area beneath the tensile curves of Figure 10 and displays an 85% fractional reduction in the aged-wet state and only a 9% recovery to unaged properties by subsequent desiccation.

Inspection of the failure surfaces by scanning electron microscopy (SEM) was undertaken and the results displayed in Figure 11. The levels of magnification in Figure 11 are indicated by the 100 μm (micron) benchmarks in the left views and the 10 μm benchmarks in the right views. The tensile fracture surfaces of unaged BP907 (upper Figure 11) show a large degree of plastic tearing combined with 5 to 10 μm spherical cavities which are evidently formed during cure of the BP907 resin. The tensile fracture surfaces of aged and dried BP907 shown in lower Figure 11 display the smoother surface characteristic of brittle fracture. The new defect structure shown in lower Figure 11 includes a whole array of microcracks with large dimensions $\geqslant 100$ μm compared to the smaller spherical cavities. The higher magnification lower right view of Figure 11 appears to present evidence for a fully three dimensional network of open and closed cracks protruding into the fracture surface. Hydrothermal aging and redrying of BP907 evidently produces a new hierarchy of micro-defects which coalesce to produce brittle failure on tensile loading with a dramatic reduction in strength, extensibility and fracture toughness.

SUMMARY AND CONCLUSIONS

This report summarizes the results of a study of hydrothermal aging (100°C in H_2O) on the epoxy matrix component of a graphite fiber reinforced composite. This study shows that the chemical mechanisms of curing and hydrothermal aging can be directly monitored by IR spectroscopy and related to network structure and states of molecular motion in the epoxy matrix phase. The specific mechanism of hydrothermal aging is shown by both IR and thermomechanical spectroscopy to modify the structure of the crosslink and introduce additional modulus changes in the low temperature (-60 to -30°C) β transition of the glass state of the epoxy resin. At room temperature the aged epoxy displays a resultant modulus decrease and increase in mechanical damping. These changes in matrix properties correlate with lowered sound velocity and increased acoustic attenuation displayed by hydrothermally aged graphite–epoxy composites studied in Part I which contain the same cured BP907 resin system.

Hydrothermal aging of cured BP907 epoxy resin is shown to produce substantially irreversible reductions in strength and extensibility of about 40%.

The combined loss of strength and extensibility produce a substantial reduction of about 75% in tensile fracture toughness. Inspection of tensile fracture surfaces indicates a loss of plastic deformation and development of a new network of micro-defects as a result of hydrothermal aging. These microstructure changes as well as degradation in modulus response at high temperature, above the epoxy glass transition temperature $T_g \simeq 122°C$, indicates that curing of the resin may result in a nonuniform network.

In general the changes in matrix properties due to hydrothermal aging parallel the mechanisms producing interfacial degradation.[5] The bulk absorption of water into BP907 is enhanced by several factors. The highly polar character of the crosslink structure, as shown in Table II, promotes a strong interaction with water. The fact that absorbed water lowers the glass-to-rubber transition to below 100°C, as shown in Figure 9, exposes the highly susceptible rubbery state of the highly crosslinked epoxy to hydrothermal aging (100°C in H_2O). Changing the curative of the BP907 epoxy resin to reduce polar character and increase the glass transition sensitivity to moisture would be expected to substantially increase hydrothermal stability in both rheological response and cohesive fracture properties.

This study shows that hydrothermal aging of a cured epoxy resin can be monitored by both chemical and physical analysis methods. It is also shown that both the interfacial and bulk matrix degradation mechanisms need to be considered as semi-independent aspects of a general environmental degradation process in fiber reinforced composites. This study, which extends the discussion of Part I on interface aspects, shows that analysis of the chemical structure and physical state of the epoxy resin phase is essential in a detailed treatment of hydrothermal aging of composite materials. The detailed information provided by interface and matrix characterization as discussed in Part I and Part II still need to be integrated into models which describe the combined constraints imposed by the interaction between fiber and matrix in the composite material. This third phase of study which forms Part III of this report emphasizes the system response properties of the composite which are sensitive to simple or combined changes in interface or matrix properties.

References

1. B. Harris, P. W. R. Beaumont and E. M. de Ferran, *J. Matl. Sci.* **6**, 238 (1971).
2. P. W. R. Beaumont and B. Harris, *J. Comp. Matls.* **7**, 1265 (1972).
3. E. L. McKague, Jr., J. E. Halkias and J. D. Reynolds, *ibid.* **9**, 2 (1975).
4. D. H. Kaelble *et al. J. Adhesion* **7**, 25 (1974).
5. D. H. Kaelble, P. J. Dynes and L. Maus, "Hydrothermal Aging in Composite Materials", to be published.
6. H. Lee and K. Neville, *Handbook of Epoxy Resins* (McGraw-Hill, New York, 1967). Pp. 4–38.

7. G. D. Wagner, Jr. and E. L. Wagner, *J. Phys. Chem.* **64,** 1480 (1960).
8. T. F. Saunders, M. F. Levy and J. F. Serino, *J. Appl. Poly. Sci., Part A-1* **5,** 1609 (1967).
9. A. F. Lewis and R. Saxon, in *Epoxy Resins,* C. A. May and Y. Tanaka, Eds. (Dekker, New York, 1973). P. 413.
10. D. H. Kaelble and E. H. Cirlin, *J. Poly. Sci., Part C* **35,** 79 (1971).
11. L. W. Crane, P. J. Dynes and D. H. Kaelble, *ibid.* **11,** 533 (1973).
12. D. H. Kaelble and T. Smith, *ibid.* **12,** 473 (1974).
13. A. S. Kenyon and L. E. Neilsen, *J. Macromol. Sci.-Chem.* **A3**(2), 275 (1969).
14. R. M. Screaton, *et al. J. Poly Sci., Part C* **43,** 311 (1973).
15. D. H. Kaelble, in *Epoxy Resins,* C. A. May and Y. Tanaka, Eds. (Dekker, New York, 1973). Chapter 5.
16. N. G. McCrum, B. E. Read and G. Williams, *Anelastic and Dielectric Effects in Polymer Solids* (Wiley, New York, 1967).
17. D. E. Kline, *J. Poly. Sci.* **47,** 237 (1960).
18. C. A. May and F. E. Weir, *SPE Technical Papers* **8,** Session 2-2, Jan. 30 (1962).